A HYBRID EDGE-CORE (3D / 1D) MODEL FOR IMPURITY TRANSPORT IN TORE SUPRA ERGODIC DIVERTOR DISCHARGES

B.Schunke, J. Hogan*, C. DeMichelis, W. Hess, M. Mattioli, J-C. Vallet

Association Euratom-CEA sur la Fusion Contrôlée, CE Cadarache, 13108 St-Paul-Lez-Durance, France.

*Fusion Energy Division, Oak Ridge National Laboratory, Oak Ridge, TN 37830, USA.

1. Introduction

Understanding the transport of extrinsic and intrinsic impurities in Tore Supra ergodic divertor (ED) discharges is needed to estimate the effect such particles have on the plasma performance. One crucial factor is the reliable description of screening processes in the scrape-off layer and edge plasma during ergodic divertor (ED) phases. Here we describe calculations made using a hybrid 3D / 1D model, coupling radial transport codes with a boundary code, and using post-process subroutines to give radial profiles of the radiated power, and of the visible bremsstrahlung and soft-X-ray emission. The corresponding measured quantities are then compared to relate the impurity density to the radiated power. The boundary conditions are found to be crucial in describing the transport processes, yet direct experimental measurements of the necessary input parameters (T_e and n_e profiles) often lack the required spatial resolution in the edge region. However, for some ED conditions T_e profiles have been measured [1], showing that increasing the divertor current sharply reduces the edge T_e, thus affecting the positioning of the radiating layers, which for light impurities lie almost entirely in the ergodic zone. Therefore a study of the coupled edge-core impurity transport has been executed, using such T_e profiles, for a sample set of auxiliary heated ED discharges with extrinsic impurities (neon, nitrogen, argon) together with the intrinsic carbon and oxygen content. We briefly describe the model for the calculations, discuss model validation using cases for which charge-exchange spectroscopy (CXS) data are available, and calculate the relation between impurity content and radiation for the sample cases.

2. Model

The calculations are made with 1D radial transport (MIST [2] and Mattioli [3]) codes and with the 3-D BBQ edge and scrape-off layer impurity transport code [4]. We distinguish a 3-D region (scrape-off layer and ergodic zone) and a 1-D region (core plasma). In the 3-D region the impurity density distributions are poloidally and toroidally asymmetric, while, in the so-called 1-D region, the densities depend only on the radial (flux surface) parameter. (Figure 1). However, with application of the ED, the 3-D region extends deeper inside the core plasma. The BBQ code is used to describe the external part of the 3-D region, to a minor radius typically chosen to be up to 5 cm inside the last closed flux surface. We describe

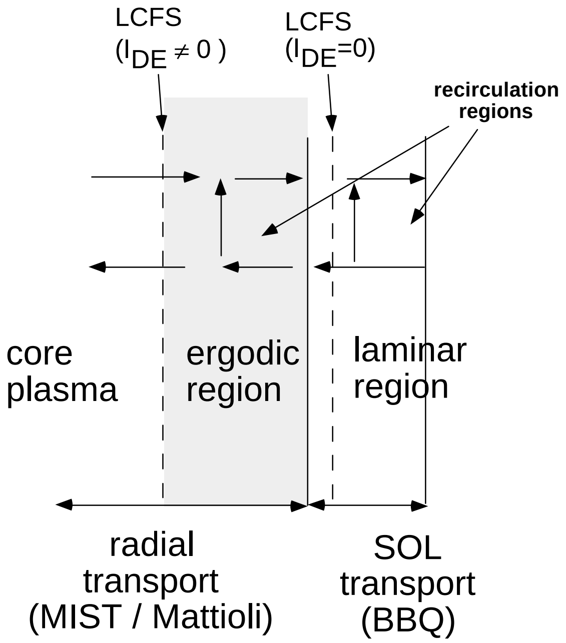

Figure 1. Schematic diagram of hybrid transport model and relevant regimes

transport in terms of effective averaged radial diffusivity D and pinch velocity V in the ergodic zone. A similar comparison was made previously using the Mattioli code in connection with earlier BBQ studies of carbon generation and transport [5]. Boundary conditions are treated slightly differently in the radial codes. For MIST the influx is distributed amongst charged ionic species with Z=2-4 for the outer 5 cm of the radius. Owing to direct core penetration as ions, rather than neutrals, this combination decreases the impurity influx needed to produce a given central concentration. In the case of the Mattioli code, in which the incoming impurities are characterised as a flux of mono-energetic neutrals incident on the last grid point, the 3-D BBQ provides the boundary condition: a neutral flux which is toroidally and poloidally averaged to make the transition to the flux-surface averaged 1-D analysis.

3. Code validation: determination of D, V for I_{DE} = 45 kA

To validate the hybrid model, transport comparisons have been made for discharges with I_{ED}= 45 kA in which CXS relative profiles have been obtained for carbon and neon [6]. The calculation for cases with CXS profiles thus allows the determination of the radial impurity transport coefficients (D, V) which are then used in the sample case study, where CXS profiles were not measured, but for which the divertor current was also I_{ED}= 45 kA. The contribution of oxygen to the radiated power is small but significant and is included. As a result of the different boundary conditions for the 1D codes, the validation

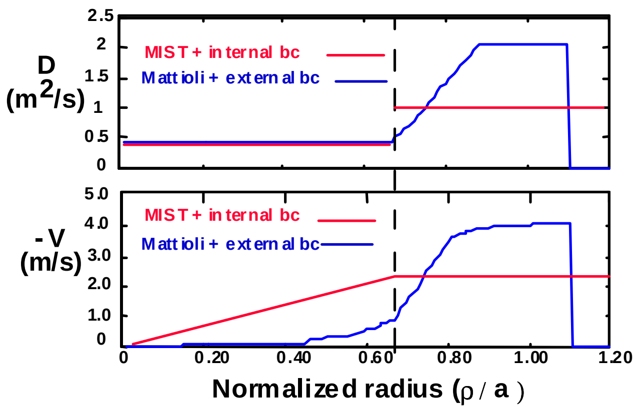

Figure 2. MIST and Mattioli code values for D, V for validation case, discharge 27845

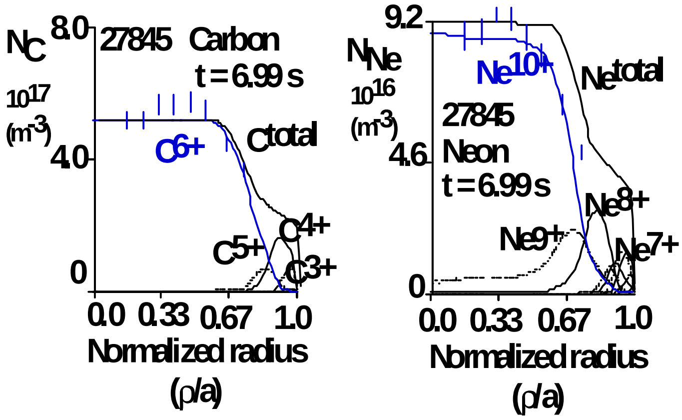

Figure 3a, b. MIST comparison with radial CXS profiles for C6+, Ne10+, discharge 27845

case gives values of D and V, which, while generally similar, have significant differences. This illustrates the role of the boundary fluxes. In the MIST case, for the reference discharge 27789 with carbon CXS profiles, the core radial time-dependent analysis finds an anomalous diffusion coefficient D = 0.335 m^2/s for ρ/a= 0.0–0.75 and D= 1 m^2 /s for ρ/a>0.75, with the inward pinch velocity V increasing from 0 to 1.4 m/s for 0<ρ/a<0.75 and V= 1.4 m/s for ρ/a>0.75. Time-dependent calculations for oxygen use the same D, V as for carbon. For pulse 27845, with both neon and carbon CXS profiles, the MIST core radial time-dependent analysis uses the same D, as for 27789, however the match to 27845 requires increasing the inward pinch velocity V with the value rising from 0 to 2.4 m/s for 0<ρ/a<0.75 and V = 2.4 m/s for ρ > 0.75. Mattioli code fits, with different boundary assumptions, find higher values of D, V, but in the same range (Fig. 2). MIST fits for the relative carbon and neon profiles at t= 6.99s are shown in Fig 3a,b.

4. Strong radiation cases

To correlate measured radiation losses with the core impurity density, as inferred from the fitting and using the model, representative pulses, all with I_{ED}= 45 kA and ICRH heating, have been analyzed. Measured time-dependent T_e and n_e profiles are used, onto which the characteristic flat ED T_e edge was modeled as the actual T_e measurements lacked the

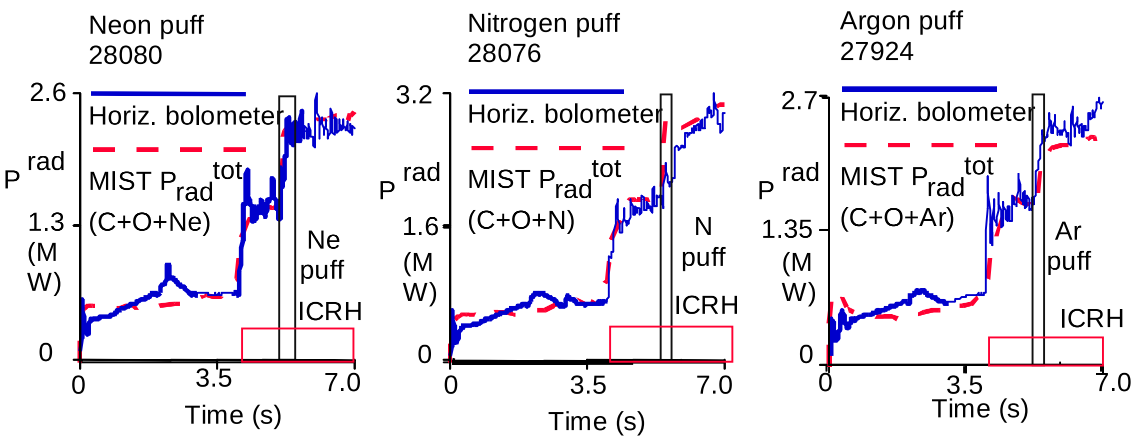

Figure 4 a-c. MIST comparisons of total radiation from C, O and injected impurity with horizontal bolometer measurement for neon (a, left), nitrogen (b, center) and argon (c, right) necessary spatial resolution to distinguish this feature. The radiative power coefficients for carbon, oxygen and neon are taken from the ADAS database (with updates by R. Dux). For argon it has been calculated using emission rates from [7] and the nitrogen radiation rates are taken from the ADPAK data included in the MIST code. Carbon, nitrogen and oxygen are assumed to be non-recycling, while neon and argon recycle with recycling coefficient R=1. In each case the background carbon and oxygen content is fit prior to the application of the ICRH heating, using the Z_{eff} increase to determine the isotopic composition between carbon and oxygen. Then the strong increase in the background radiation due to the increase in carbon content from the ICRH heating is matched, and after that the additional radiative power produced by the injected impurity is matched. With this matching, using the transport coefficients previously obtained, we thus obtain a reasonable estimate for the core impurity content for the cases listed in the Table. Figure 4a-c shows the time-dependent comparison of MIST results with the measured total radiation for three of these pulses to demonstrate the good agreement between the simulations and the experimental data. For each of these cases the central impurity density, N_Z (0), the impurity density at the radial location of the maximum local radiated power density, $N_Z^{rad\ Max}$, the maximum local radiated power density, the values of T_e and n_e in the center and the values at the radial location of maximum radiated power density ($T_e^{rad\ Max}$ and $n_e^{rad\ Max}$) have been evaluated and are also shown in the Table. Such a technique is complementary to the direct measurement of central impurity content by charge exchange recombination techniques.

Table Relation between core impurity density and radiated power

Shot	Impurity	N_Z (0) (10^{17} m^{-3})	$N_Z^{rad\ Max}$ (10^{17} m^{-3})	P_{rad}^{Max} (MW / m^3)	$T_e(0)$ (keV)	$T_e^{\ rad\ Max}$ (keV)	$N_e(0)$ (10^{20} m^{-3})	$N_e^{\ rad\ Max}$ (10^0 m^{-3})
28080	Neon	1.29	0.55	0.60	3.00	0.086	0.38	0.19
28081	"	1.97	0.84	0.69	3.37	0.080	0.41	0.17
28076	Nitrogen	1.88	0.90	0.85	2.43	0.091	0.57	0.28
27924	Argon	0.42	0.21	0.56	3.68	0.088	0.41	0.20
27928	"	0.91	0.46	0.73	2.40	0.089	044	0.19

References

1. M. Becoulet et. al. Contrib. Plasma Phys. , **40**, 251 (2000)
2. R. Hulse Fusion Technology / Fusion **3**, 259 (1983)
3. M. Mattioli et. al., Nucl. Fus. **38**, 1629 (1998)
4. J. Hogan et al, J. Nucl. Mater. **290-293**, 628 (2001)
5. S. Tobin et. al. Plas. Phys. Cont. Fus. **38**, 251 (1996)
6. W. Hess et. al., Proc. of the 27th EPS Conf. Budapest 2000, ECA Vol. **24B**, 612 (2000)
7. K. Fournier et al, At. Data Nucl. Data Tables **70**, 231 (1998)